**Cell, Volume *136***

# Supplemental Data

# The Role of the Granuloma in Expansion and Dissemination of Early Tuberculous Infection

**J. Muse Davis and Lalita Ramakrishnan**

## Supplemental Figures

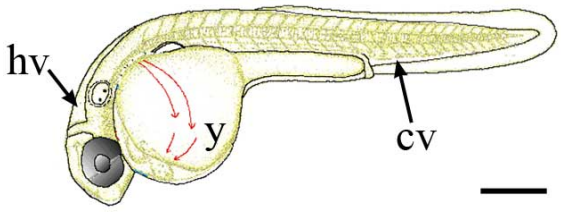


**Figure S1**
Overview of zebrafish embryo anatomy. cv: caudal vein, hv, hindbrain ventricle, y, yolk. Scale bar, 300μm.

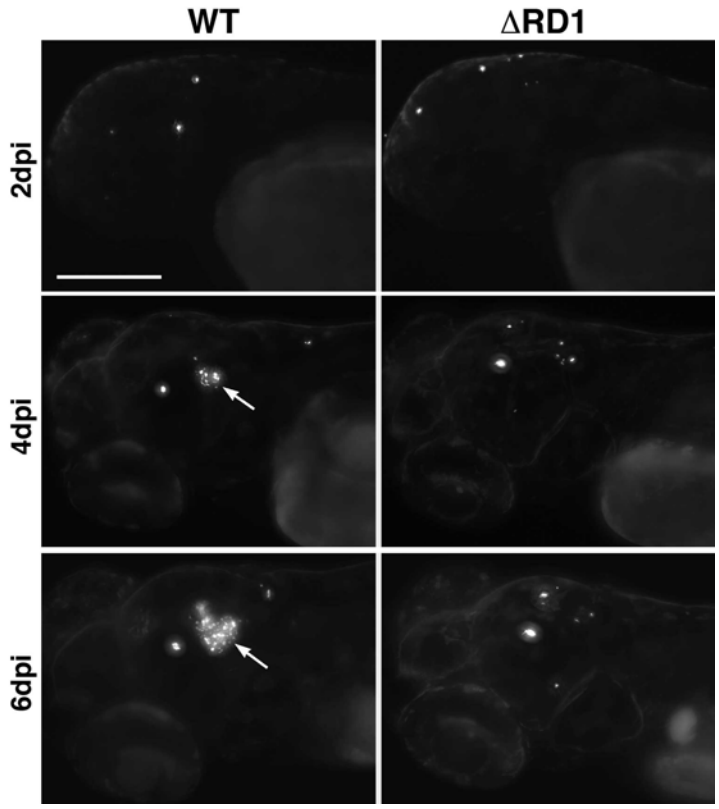


**Figure S2**

Overall progression of infection after hindbrain ventricle injection of 50-100 CFU of WT (left) or ΔRD1 (right) Mm. Though the burden of bacteria at 2dpi appears similar, the advent of a granuloma (arrows) in WT by 4dpi results in dramatically greater bacterial numbers by 6dpi. All bacteria present in these animals were only found in the head (data not shown), thus granuloma formation does not proceed from recruitment of infected cells. Scale bar, 200μm.

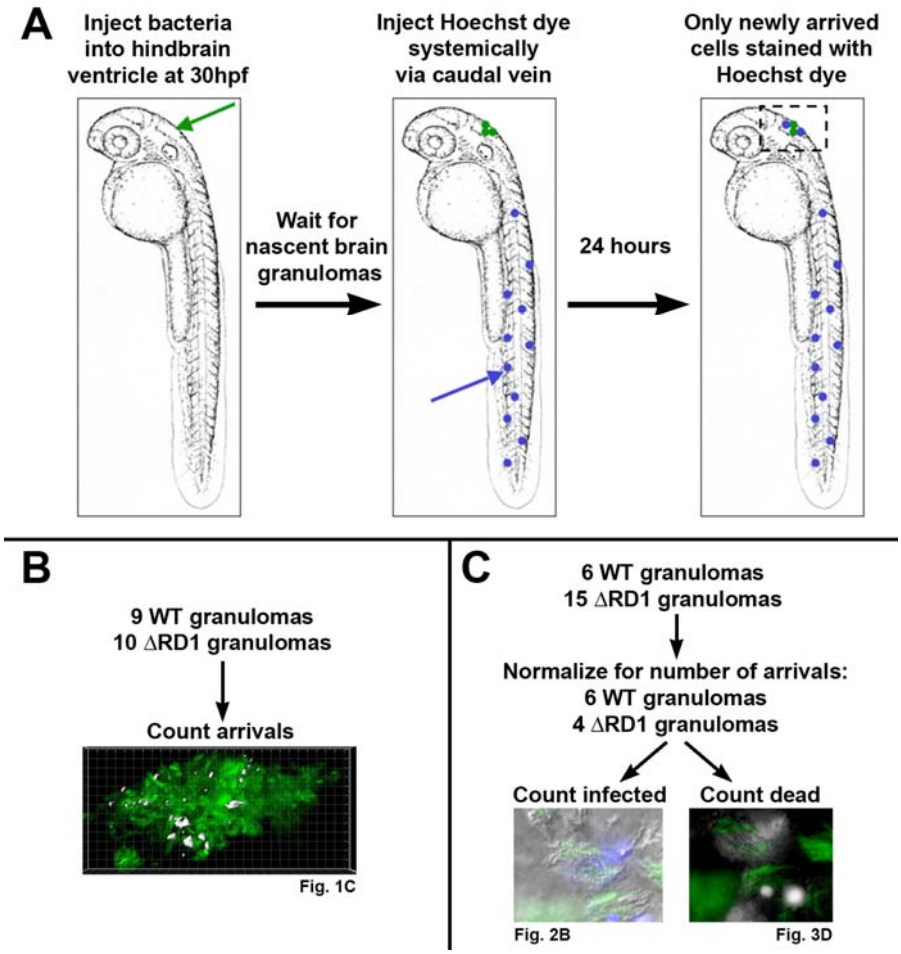


**Figure S3**

Experiment to enumerate and characterize macrophages newly arrived to a granuloma within 24 hours. (**A**) Outline of injections. Bacteria are injected into the hindbrain ventricle at 30 hours post fertilization (hpf). In order to form infected lesions large enough to compare with WT bacteria, ~5x the dose of ΔRD1 was used (50-100 in WT vs 250-500 in ΔRD1). Nascent brain granulomas usually appear two to three days post infection (dpi). At this point embryos with nascent granulomas are injected via tail vein with Hoechst 33342 nuclear dye, which stains the nuclei of cells in the blood and many tissues, but not the brain (data not shown). (B-C) Outline of counting and analysis. (**B**) At 24 hours after the Hoechst injection, the granulomas are imaged to quantitate the number of cells recruited. See Figure 1C-E. (**C**) To study the fates of arrived macrophages, a second set of granulomas was analyzed. Embryos were injected as before, but a subset of granulomas with no significant difference in arrival number were analyzed. (WT: 39.3+/- 13.6, ΔRD1: 30.0 +/- 12.99, p=0.312). (Analysis of this subset or of all granulomas yielded the same results). 3D DIC timelapse was used in addition to widefield fluorescence to allow positive identification of infected state. See Figure 2A-C. Collapsed nuclei have a distinct fluorescent appearance, but were cross-checked with DIC footage as well. See Figure 3D-E.

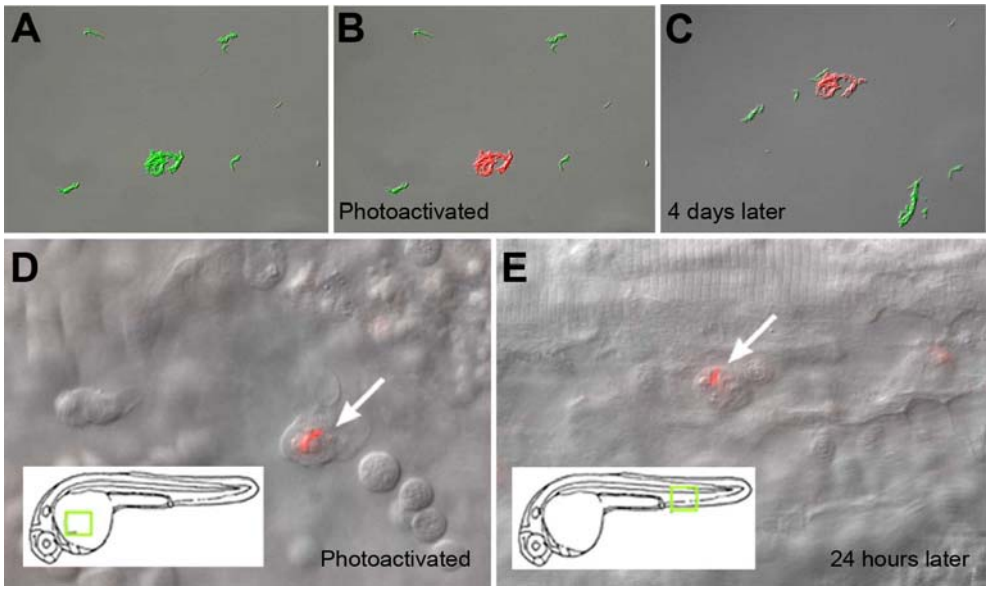


**Figure S4**

*M. marinum* expressing Kaede photoactivatable protein to mark and track infected macrophages in vivo. (**A**-**B**) Merged image of photoactivated (red) and non-photoactivated (green) bacteria in medium immediately before (A) and after (B) photoactivation. (**C**) Same bacteria still detectable four days later. (**D**) Single macrophage containing photoactivated *M. marinum* (red channel only) in yolk circulation valley of embryo, immediately after photoactivation. (**E**) The same bacteria detected 24 hours later in caudal vein. Insets show location in embryo.

**Mathematical modeling of the role of macrophage death in granuloma growth.**

To establish a simple model for granuloma expansion, we started with a series of assumptions, supported by our experimental results. The most important are: 1) granuloma growth can be measured by an increase in the number of infected macrophages (Figure 4 B, D), 2) apoptotic bodies are stable for at least 24 hours and are left behind by all infected macrophage deaths, and 3) the live bacterial contents of dead macrophages may be phagocytosed either whole or in part by either infected or uninfected macrophages. We reasoned that the number of infected macrophages present at 24 hours ($N_{24}$) must be a function of the number present at time 0 ($N_0$). Some fraction (*f*) of $N_0$ will die during the 24-hour period, and their bacterial contents will be taken up by a number (*m*, for multiplicity) of new macrophages. Therefore the dying macrophages will result in a new number of infected macrophages which equals $N_0(fm)$. This number, plus the number of infected macrophages not dying ($N_0(1-f)$) will total the number of infected macrophages present at 24 hours, as shown in equation 1.

$$N_{24} = N_0\left[fm + (1-f)\right] \quad (1)$$

Rearranged to express proportional growth of the granuloma in terms of infected cells ($N_{24}/N_0 = G$), this becomes:

$$G = f(m-1)+1 \quad (2)$$

We propose that the major mechanism for cell-to-cell bacterial spread in nascent granulomas is the apoptotic death of infected macrophages followed by the phagocytosis of these cells and their bacterial cargo by one or more other macrophages. In order to estimate the relative importance of this mechanism to the increase in the number of infected cells in a growing granuloma, we formed single brain granulomas in five different embryos and imaged each at time 0 (when the granulomas were still relatively small) and 24 hours later. Because granulomas near the hindbrain ventricle tend to be planar in shape, we first used a simple measure of bacterial fluorescence area in a flattened image to estimate granuloma size and growth. Next, the fluorescence datasets were deconvolved and analyzed in three dimensions in order to estimate the number of infected macrophages (discrete clusters of bacteria) present at both timepoints. Finally, high resolution DIC stacks taken at the same timepoints allowed the detection and enumeration of apoptotic bodies, which serve as effective markers of previous apoptosis events (Figure 3F-I). In cases of fragmentation of apoptotic bodies (as in Figure 3B), we counted clustered fragments as a single apoptotic event. The results of these measurements are summarized in Table S2.

We reasoned that if the proposed mechanism was the only one responsible for expansion in the number of infected cells, the change in cell number over 24 hours could be predicted based upon the number of infected macrophages present at time zero, provided the fraction of cells that die per unit time (*f*) and the multiplicity of infection (*m*) are known (see text). The

assumptions we made in designing the model, and the rationale for each, are displayed in Table S1.

Given Equation 2 and the data from before and after a 24 hour period of granuloma expansion (Table S2), we had the data necessary to calculate values for *f*, *m*, and G as well as the opportunity to use calculated values of f and m to derive a predicted value for G. We reasoned that comparing this predicted G to the measured G would provide an estimation of the percentage of actual granuloma expansion that could be explained by the proposed mechanism operating according to the proposed model.

Estimation of *f*, the fraction of infected cells present at time 0 which die by 24 hours:

For each embryo, the number of new apoptotic bodies formed would be equal to the number of original infected macrophages which had died. Therefore *f* could be calculated by:

$$f = \frac{A_{24} - A_0}{N_0} \quad (3)$$

Where:

$A_0$ = apoptotic bodies present at time 0

$A_{24}$ = apoptotic bodies present at 24 hours

$N_0$ = infected cells present at time 0

Calculating *f* for all five fish resulted in a mean of 0.77 (+/- 0.12).

Estimation of *m*, the number of new infected macrophages resulting from a single apoptotic event:

Based on our assumptions and the observations we had made of single or multiple macrophages engulfing the remains and bacteria from infected macrophages, we expected this number to be greater than one and perhaps as high as three or four. We used the following formula to derive a measured *m* from the infection data:

$$m = \frac{N_{24} - N_0}{A_{24} - A_0} \quad (4)$$

Where $N_{24}$ = infected cells present at 24 hours.

The value for G is defined as $I_{24}/I_0$.

The resulting actual and predicted values for G for each embryo are listed in Table S3. As mentioned in the text, the results suggest that this mechanism accounts for a large majority of granuloma expansion. Our model does not account for possible positive feedback in the system, which would mean the entire effect of the process is amplified as time goes by, since more infected cells are present over time. This effect may well account for the rest of the observed granuloma expansion, but since we do not have a good estimate of the

magnitude of this effect, we have chosen the conservative stance of leaving it out. Given the extreme simplicity of our model, this analysis only vouches for the plausibility of our proposed mechanism being the major factor in granuloma expansion. The results leave room for additional mechanisms, but can also account for our proposed mechanism being the only one.

## Supplemental Experimental Procedures

### Bacterial Strain Production

Kaede-expressing Mm was prepared as follows: The Kaede ORF was PCR amplified from the –pKaede-MC1 plasmid (MBL Int. Corp.) using the primers KaedeProkF (5'-CCCGGTACCAGATCTTTAAATCTAGATTTAGAAGGAGATATACATATGGTGAGTCTGATT-3') and KaedeProkR (5'-GATCGCTAGCAGTTACTTGACGTTG-3'). The product was then cleaved with KpnI and NheI and cloned into pMSP12::gfp (Chan et al., 2002), which was similarly digested to remove the gene encoding Green Fluorescent Protein (gfp). This resulting plasmid, bearing Kaede driven by msp12, was named pMSP12-Kaede. Mm transformed with p-msp12-Kaede was named MD2.

### Mounting of Embryos for Timelapse Microscopy

Embryos imaged for two hours or less were immobilized in 1.5% low melting point agarose on glass cover slips and covered in fish water with tricaine (as per (Cosma et al., 2006; Davis et al., 2002). For long-term timelapse (up to 18 hours) embryos were similarly mounted in a chamber based on that described by Kamei et al (Kamei et al., 2004; Kamei and Weinstein, 2005) but modified for use with an inverted confocal microscope, with ~30ml of tricaine/fish water and no recirculation.

### Image Analysis

Tracking of cells in DIC was performed in Imaris by visualizing DIC planes in Ortho Slice mode and creating spots at the estimated centroid of the nucleus at each time point. Bacterial volumes were estimated in Imaris either by calculation of fluorescence volume or by calculation of surfaces traced manually over DIC images. Area measures of granuloma fluorescence were performed in MetaMorph by collapsing fluorescence z-stacks using maximum intensity projection to produce a 2D image. The image was the thresholded to exclude background light intensities and the total area above threshold measured.

# Supplemental Tables

## Table S1

Assumptions used for mathematical modeling of granuloma expansion

| Assumption | Rationale |
|---|---|
| Granuloma growth can be measured by increase in the number of infected macrophages. The supply of new cells is provided by constantly arriving uninfected macrophages. | Figure 1B shows the typical expansion mode, with distinct additional clusters of bacteria rather than the expansion of a monolithic cluster. Figure 4A shows the evidence that rapid recruitment of new cells correlates with expanding WT granulomas. Infected cells have been shown to be incapable of dividing in granulomas (Dannenberg, 2003). |
| All infected macrophage deaths are rapid and apoptotic, always leaving behind apoptotic bodies which are stable for at least 24 hours. | The rapid course of nuclear collapse and apoptotic body formation is illustrated in Figure 2B and Movie S3. Figure 3D-I details the accumulation of apoptotic bodies over 24 hours and the correlation of the DIC appearance of apoptotic bodies with molecular markers of apoptosis. |
| Dead infected macrophages may be engulfed either whole or in part by either infected or uninfected macrophages. | Figure 3C and Movie S5 show the engulfment of a whole dead macrophage by a single cell, and Figure 3J and Movie S6 show an example of the partial engulfment of the bacteria of an infected cell while the rest is engulfed by another. We have also collected video evidence of up to four macrophages sharing the bacteria of a single dead cell (data not shown). |
| When an apoptotic body is engulfed, it is taken up entirely by one macrophage, while the bacterial contents of the cell may be shared among multiple macrophages. | The events of Figure 3J and Movie S6 support this phenomenon, and other data not presented suggest that phagocytosis by multiple cells generally involves one major but incomplete phagocytosis, with smaller portions of the contents rapidly taken up by other nearby cells. |
| All observed apoptotic bodies are within macrophages. | Figure 3B and C picture the same cell undergoing death and engulfment over the course of 46 minutes. Timelapse of these events is shown in Movies S4 and 5. Based on this and similar observations not shown, we surmise that a dead cell spends very little time before being phagocytosed. |
| Infected macrophages depart rarely. | Instances and frequency of infected cell departure are addressed in Figure 5. In the context of a large number of infected macrophages in a growing granuloma, we find the impact of these departures on overall growth to be negligible. |

**Table S2**
Measurements of expansion and apoptosis in a granuloma over 24 hours.

| Embryo* | Area of bacterial fluorescence ($\mu m^2$), time 0 | Area of bacterial fluorescence ($\mu m^2$), 24 hours | Infected cells, time 0 | Infected cells, 24 hours | Apoptotic bodies, time 0 | Apoptotic bodies, 24 hours |
|---|---|---|---|---|---|---|
| 1 | 1473 | 2636 | 40 | 76 | 13 | 38 |
| 2 | 1693 | 3883 | 33 | 94 | 24 | 57 |
| 4 | 950 | 4746 | 36 | 87 | 24 | 48 |
| 5 | 969 | 3665 | 29 | 86 | 15 | 39 |
| 8 | 912 | 2095 | 18 | 68 | 13 | 26 |

*Embryo numbers are discontinuous--starting from nine embryos, some were lost to handling or were excluded when DIC imaging proved too poor to enumerate apoptotic bodies.

**Table S3**
Observed and calculated growth, death fraction, and multiplicity of infection in 24 hour granulomas.

| Embryo | Observed G from fluorescence area | Observed G from infected cell counts | Predicted G | Calculated *f* | Calculated *m* |
|---|---|---|---|---|---|
| 1 | 1.8 | 1.9 | 1.3 | 0.6 | 1.4 |
| 2 | 2.3 | 2.8 | 1.8 | 1.0 | 1.8 |
| 4 | 5.0 | 2.4 | 1.7 | 0.7 | 2.1 |
| 5 | 3.8 | 3.0 | 2.1 | 0.8 | 2.4 |
| 8 | 2.3 | 3.8 | 3.1 | 0.7 | 3.8 |
| **Average** | **3.0** | **2.8** | **2.0** | **0.8** | **2.3** |
| SEM | 0.6 | 0.3 | 0.5 | 0.1 | 0.6 |

**References**

Dannenberg, A. M., Jr. (2003). Macrophage turnover, division and activation within developing, peak and "healed" tuberculous lesions produced in rabbits by BCG. Tuberculosis (Edinb) *83*, 251-260.